HIGH-FIDELITY FE MODELLING OF Z-PINS IN QUASI-ISOTROPIC LAMINATES

B. Zhang [a*], G. Allegri [a], S. R. Hallett [a]

[a] *Advanced Composites Centre for Innovation and Science (ACCIS), University of Bristol, Queen's Building, University Walk, Bristol, BS8 1TR, UK*
[*] *B.Zhang@bristol.ac.uk*

Keywords: Z-pinning; Delamination; Fracture; Finite element analysis (FEA)

Abstract
This paper presents a three-dimensional FE modelling approach to simulate the mechanical response of individual Z-pins at the micro-scale and the associated bridging mechanism. This modelling strategy accounts for the characteristic features associated with Z-pinning, i.e. the interface between Z-pin and the surrounding laminate block, residual stresses due to the post-cure cool down and split within the Z-pin. The Z-pin failure is described using the Weibull's failure criterion. The analysis results are in excellent agreement with the experimental results from tests performed on single Z-pinned quasi-isotropic coupons. The analyses demonstrate that the de-bonding of the Z-pins from the laminate is essentially due to thermal residual stresses. For both Mode I and Mode II loading cases, enhanced friction zones develop along the Z-pin. This is the main cause of the progressive split between fibre strands in Mode II. The split initiates at the Z-pin centre and then propagates along the neutral plane. The modelling strategy presented in this paper can be directly extended to arbitrary stacking sequences as well as asymmetric insertion cases.

1. Introduction

Through-thickness reinforcement of composite laminates via Z-pinning yields large increases of interlaminar fracture toughness. Several modelling approaches have been developed to predict the fracture toughness enhancement due to through-thickness reinforcement. Cox introduced an analytical model for Mode II bridged delamination and then generalized his approach to a Mixed-Mode loading condition [1,2]. Cox's models give the relation between the bridging traction and crack open/sliding displacement as an implicit function. Allegri and Zhang proposed an explicit micro-scale model for the response of single Z-pins. Explicit models, i.e. those yielding the bridging tractions as a function of the delamination opening/sliding displacement, are easier to implement in FE analysis [3]. To study on the Z-pinned laminates, the behaviour of single Z-pins has also been described employing non-linear spring elements in the framework of FEA [4].

However, more robust high-fidelity models are still needed for understanding the mechanical response of the Z-pin and the embedding blocks (resin and laminates) for different delamination scenarios and stacking sequences. This article presents a three-dimensional FE modeling approach to model the mechanical response of individual Z-pins at the micro-scale.

The micro-structures of Z-pinned laminates is represented in detail. The simulation results for Z-pins in quasi-isotropic laminates subject to Mode I and Mode II loading are in good agreement with experimental data.

2. Modelling strategy

2.1. Ply level mesh

A star-like ply level mesh in Figure 1 (a) is employed to simulate the micro structure of Z-pinned laminate [5]. This accounts for relative orientation of the resin pockets surrounding Z-pin in -45°, 0°, 45° and 90° lamina as well as the in-plane misalignment of the laminate fibres due to the presence of the Z-pin [6]. The Z-pin misalignment in the through-thickness direction can also be modelled as shown in Figure 1 (b).

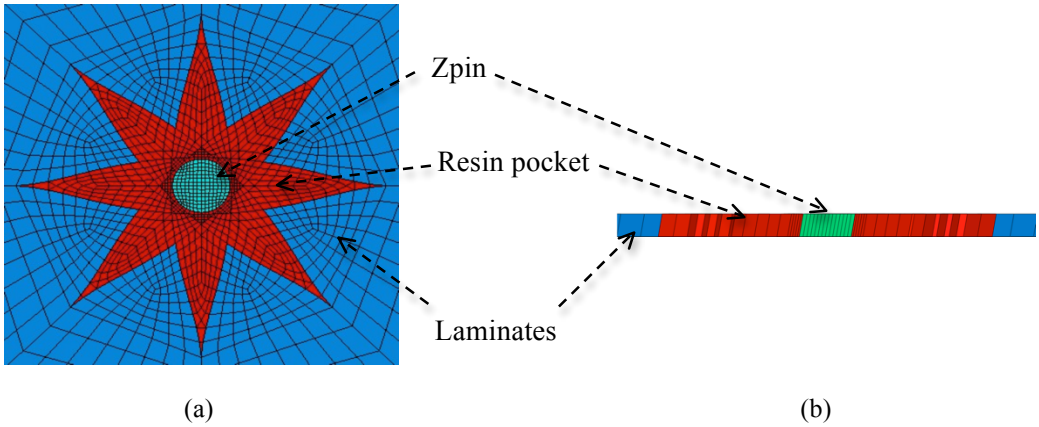

Figure 1. (a) Ply level mesh of Zpinned laminates. and (b) Zpin misalignment.

In this study, the Z-pin diameter is 0.28mm. The in-plane fibre misalignment is described by Eq. (1).

$$\theta = -8 \bullet \frac{0.4 - |y|}{0.4} \bullet \frac{x}{1.0} \bullet \mathrm{sgn}(\frac{x}{y}), \tag{1}$$

which has been calibrated on micro graphs taken on single Z-pin coupons [7]. In Eq. (1), x is the distance between the centroid of each individual element and the Z-pin centre along the length of the resin pocket. Similarly, y is the distance between the element centroid and the Z-pin centre with respect to the resin pocket width.

The Z-pins considered here were manufactured via pultrusion of uni-directional carbon fibre tows impregnated with bismaleimide (BMI) resin [8]. If high longitudinal-transversal shear stress are attained, the Z-pin is susceptible to split into strands that can slide along each other to accommodate further loading before failure [1]. In the 3D FE modelling, split is assumed to occur only in the planes normal to the Z-pin lateral displacement. The in-plane mesh of Z-pin is shown in Figure 2. Columns of zero-thickness cohesive elements are inserted within Z-pin as seeds for the splits. These cohesive elements follow the bi-linear cohesive law [9]. Once these cohesive elements fail, the exposed surfaces are assumed to experience Coulomb frictional contact, with maximum frictional stress capped at 25 MPa. The split modelling parameters are listed in Table 1.

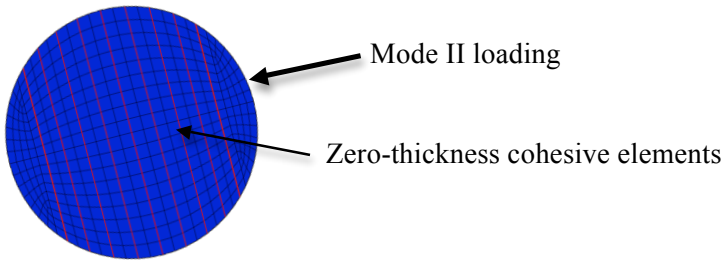

Figure 2. Mesh of Z-pin with split cohesive elements.

	Split behaviour	**Zpin/laminate interface**
$\sigma_{I,max}$(Mpa)	90	30
$\sigma_{II,max}$(Mpa)	110	60
K_I(N/mm3)	1.0e5	1.0e5
K_{II}(N/mm3)	1.0e5	1.0e5
G_{IC} (N/mm)	0.2	0.01
G_{IIC} (N/mm)	0.8	1.0
α	1	1
μ	0.3	0.8
$\sigma_{t,max}$(Mpa)	25	60

Table 1. Parameters of split behaviour and Zpin/Lamina interface.

The interface between the Z-pin and the surrounding laminate blocks is also modelled using a bi-linear cohesive law, which has been implemented by defining a cohesive contact behaviour in Abaqus/Explicit. The initial debonding is followed by Coulomb frictional stage with maximum stress capped at 40MPa. The interface modelling parameters are listed in Table 1.

2.2. Material definition

Linear-elastic orthotropic material properties are employed to model both the laminate and the Z-pin. The neat resin is modelled as an isotropic elasto-plastic material with plastic stress as 104Mpa. The associated properties are listed in Table 2.

	Laminate (IM7/8852)	**Z-pin (T300/BMI)**	**Resin (8552)**
Young modulus, E_l(Gpa)	161	144	4.67
Young modulus, E_t (Gpa)	11.38	7.31	
Shear modulus, G_{lt} (Gpa)	5.17	4.45	1.73
Shear modulus, G_{tt} (Gpa)	3.98	2.63	
Poisson's ratio, v_{lt}	0.32	0.25	0.35
Poisson's ratio, v_{tt}	0.436	0.39	
Thermal coefficient, α_{tt}($^oC^{-1}$)	3.0e-5	3.0e-5	7.5e-5
Thermal coefficient, α_{ll}($^oC^{-1}$)	0	0	

Table 2. Properties of laminate, Z-pin and resin.

The Z-pin strength is described by using a classical two-parameter Weibull's cumulative distribution, which is based on the assumption that only axial tensile stresses govern the Z-pin

failure [10]. The two-parameter Weibull's model states that the probability of survival under a stress field is:

$$P(s) = \exp[-\int (\frac{s}{s_0})^m \, dv] \tag{2}$$

where s_0 is the characteristic strength (or scale parameter) and m is the Weibull modulus (or shape parameter). Using the assumption of equal probability of survival for individual volumes within the Z-pin and an ASTM standard tensile test one finds

$$\exp[-V_E(\frac{s_E}{s_0})^m] = \exp[-V_{ASTM}(\frac{s_{ASTM}}{s_0})^m] \tag{3}$$

where V_E is the volume of individual element. S_E is the fibre-direction tensile stress in the element. V_{ASTM} is the volume of standard ASTM sample, 2250mm^2. S_{ASTM} is the unidirectional failure stress of standard ASTM sample, 1800Mpa; m is assumed to be 25.

From Eq. (3), it is straightforward to derive the following strength scaling criterion

$$\frac{V_E}{V_{ASTM}}(\frac{s_E}{s_{ASTM}})^m = 1, \tag{4}$$

which has been implemented in a VUMAT subroutine of Abaqus/Explicit.

2.3. Full Model and analysis steps

The FE analysis strategy outlined above was applied to single Z-pins embedded in quasi-isotropic laminates. As validation cases, we consider the single Z-pin experimental tests performed in [7]. The laminate stacking sequence was $[(0/45/90/-45)_{4s} // (90/-45/0/45)_{4s}]$. The coupons consisted of two symmetric blocks separated by an artificial delamination. The blocks were bridged by a single Z-pin located at the centre of the coupon. Each block was manufactured using 32 plies of IM7/8552 (Hexcel, UK). Each lamina had the nominal thickness of 0.125mm. The full FE model built in Abaqus was generated by stacking ply level meshes together, as shown in Figure 3. The mesh was finer in close to the fracture plane (8 elements per ply in the through-thickness direction). This mesh refinement was introduced in order to capture the stress concentrations due to the local friction enhancement in mode II.

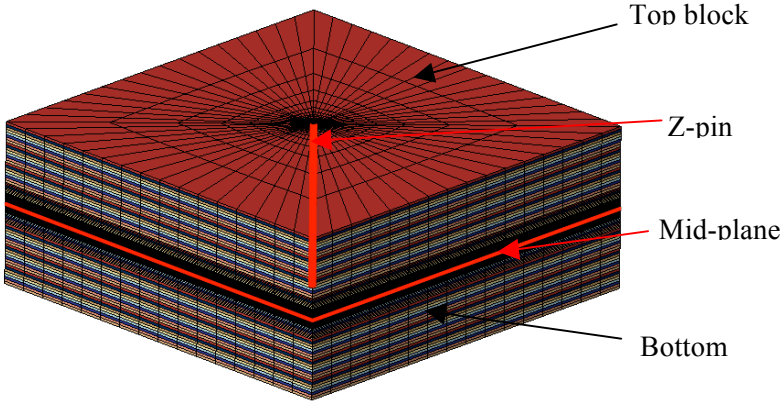

Figure 3. Full FE model of Zpinned quasi-isotropic laminates.

The full analysis consists of two analysis steps, namely cure (thermal) and pull-out (mechanical). In the cure step, a temperature field representing a post-cure -160°C cool-down is imposed to all the nodes of the model. In the pull-out step, the boundary condition depends on the actual mode mixity. By taking the nominal mode mixity and Z-pin misalignment angle into account, the actual mode mixity is defined as:

$$\phi = \sqrt{\cos^2\chi\sin^2\zeta + \sin^2\chi(\sin^2\psi + \cos^2\psi\cos^2\zeta) - \frac{1}{2}\sin 2\chi\sin 2\zeta\cos\psi} \tag{5}$$

where χ is the nominal mixed mode angle, ζ the pin misalignment angle from pin-axis, ψ the in-plane deviation of pin from x-axis [7].

For the mode I cases, a pull-out velocity is applied on the top surface of top block while bottom surface of bottom block is fully constrained. For the Mode II loading case, a velocity is applied on one lateral surface of top block while opposite lateral surface of bottom block is constrained in the sliding direction. The velocities applied in the axis direction and shear direction are defined as:

$$\begin{bmatrix} V_{axis} \\ V_{shear} \end{bmatrix} = 0.1 \begin{bmatrix} \cos(\tan^{-1}(\frac{\phi}{\sqrt{1-\phi^2}})) \\ \sin(\tan^{-1}(\frac{\phi}{\sqrt{1-\phi^2}})) \end{bmatrix} \text{ mm/s} \tag{6}$$

3. Modelling Results

3.1. Post-cure cool down

One main effect of the post-cure cool-down is the debonding of the Z-pin from the laminate. The analysis indicates that the debonding starts on the surface of the Z-pin that faces the resin rich region, since this corresponds to the largest mismatch of thermal expansion coefficients. However, the debonding progresses in a helix path due to the different ply orientations through the thickness. The complete failure of the Z-pin/laminate interface occurs at the end of the thermal step, as already observed in the literature [11]. This also agrees with the reported lack of a mechanical debonding stage for Z-pin in non-UD laminates [12]. This phenomenon is also confirmed in the simulated pull-out step, where there is no peak force associated with debonding.

The other effect of cure cool-down is the accumulation of damage in the cohesive elements that represent the Z-pin splits. This makes the Z-pin weaker upon the application of a delamination sliding displacement, i.e. the post cure cool-down promotes split in the subsequent pull out step.

3.2. Mode I loading

A snapshot of the stress field during the Z-pin pull-out shown in Figure 4 (a). The stress distribution confirms that Mode I loading is actually a mode I dominated mixed-mode regime due to the Z-pin misalignment. The enhanced friction zone appears in two areas, geometrically opposite to each other. Both propagate with an increasing opening displacement. This phenomenon is denoted in the literature as “snubbing” effect [13]. Due to low mode mixity, no splits were observed. From the “Stress 11” contour plotted on the pin, the maximum tensile stress is always located opposite to the enhanced friction region. This indicates that the Z-pin failure is mode-mixity driven, as reported in [7].

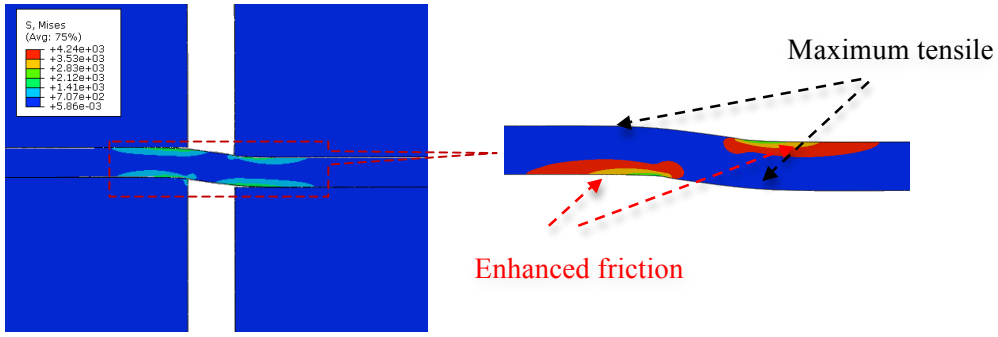

(a) (b)

Figure 4. (a) Pull-out of Zpin and (b) Enhanced friction zone.

In Figure 5, the pull-out traction-displacement curves from the FE simulations are compared to the experimental results. The experimental data are given in terms of average load-displacement curves and the associated standard deviation. Five single load-displacement traces were considered.

Figure 5 also shows that the FE results agree well with the experimental tests for QI single Z-pin coupons. As mentioned above, it is worth noticing that the load-displacement traces do not display the debonding peak load observed in the UD case. In other words, frictional forces govern the Z-pin pull-out in QI laminates, with negligible influence of progressive debonding. This result is here explained by considering the thermal residual stresses that arise during the post-cure cool-down. The FE results presented here provide a better fit of the load-displacement curve than previous models where a constant additional shear stress is added on standard Coulomb friction [11]. However, the peak force value is similar. Overall, this implies that enhanced friction plays a crucial role in the delamination suppression via through-thickness reinforcement.

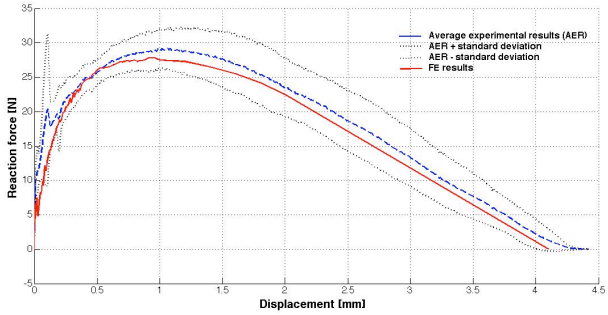

Figure 5. Reaction force vs. displacement curves of Z-pin pull-out.

3.3. Mode II loading

For Mode II loading, the two blocks slide with respect to each other with the increased loading. This implies that opposite frictional stresses are applied on the two anti-symmetric enhanced friction zones. Split initiates from the Z-pin neutral plane. Here the neutral plane is the plane that contains the Z-pin axis and it is normal to the mode II sliding. Increasing the loading, the split propagates along the neutral plane and until the final Z-pin rupture occurs because of tensile fibre failure.

Figure 6 (a) shows that Z-pin failure initiated from the areas opposite the enhanced friction zone. The maximum tensile stress corresponding to the failure initiation is 3553 Mpa. The

corresponding split configuration is shown in Figure 6 (b).

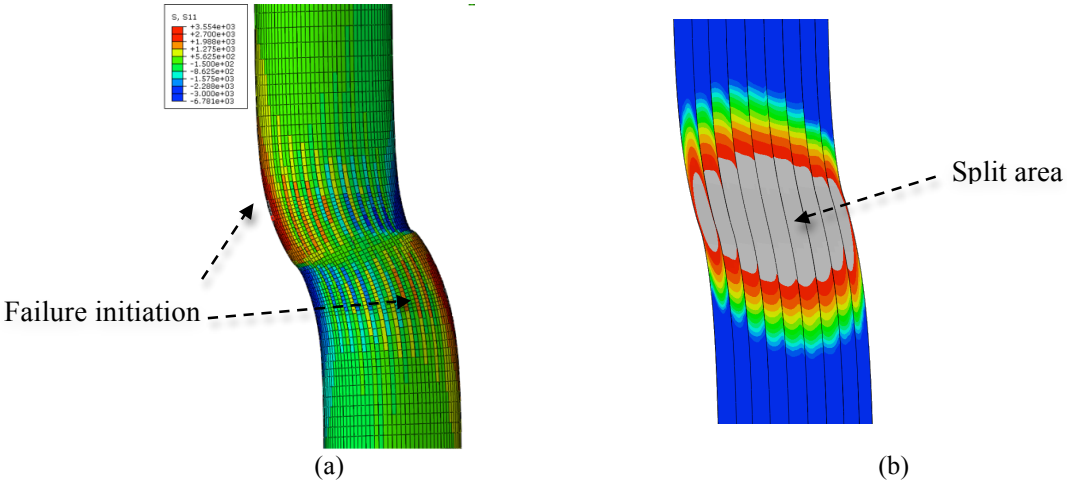

Figure 6. (a) Zpin failure initiation and (b) Corresponding split status.

In Figure 7, the Mode II traction-displacement curve from the FE simulation is compared to the experimental result. The model provides a correct estimation of the peak force and deformation corresponding to the pin rupture. This implies that predicted fracture toughness due to Z-pinning gives excellent agreement with experiment. The simulations show that, upon the application of an increasing load, extensive splitting of the Z-pin occurs close to the delamination plane. However the failure is still governed by the tensile strength of the fibres, which can carry load even in presence of splitting. The final load drop occurs when the fibres fail as predicted by the Weibull's criterion.

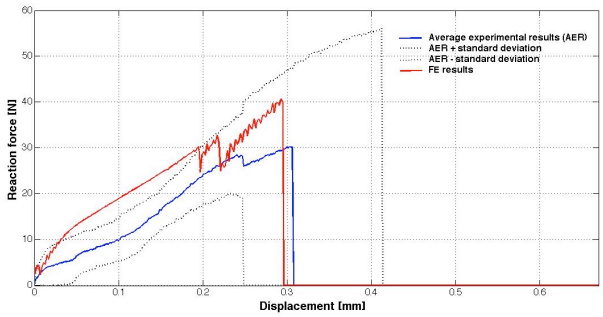

Figure 7. Reaction force vs. displacement curves in Mode II.

4. Concluding remarks

A micro-mechanical analysis of single Z-pin delamination bridging has been carried out by employing high-fidelity ply-level meshes, which explicitly describe the micro-structure of Z-pinnned laminates, including the resin pocket, the fibre in-plane waviness and the Z-pin misalignment. The interface between Z-pin and laminate has been modelled using cohesive contact enhanced by Coulomb friction. The Z-pin failure is described by using a Weibull's failure criterion.

The analysis results indicate that the bonding between pin and the embedding quasi-isotropic laminate fails due to the thermal residual stresses caused by post-cure cool down. The bridging forces obtained for Mode I and Mode II regimes are in good agreement with experimental results. The enhanced frictional contact in mode I dominated loading is

essentially due to the Z-pin misalignment. For the Mode I loading case, the pull-out reaction force gives the same peak force as past models in the literature [11]. This implies that the enhanced friction contact is the main factor controlling the Z-pin bridging in Mode I. However, the model proposed here gives a better prediction of the actual load-displacement trend. For the Mode II loading cases, split initiates at the Z-pin neutral plane and then progressively propagates until the final Z-pin rupture. The Z-pin failure initiates from the areas geometrically opposite to the enhanced friction zones and cut across the through thickness reinforcement at the delamination plane.

This modeling strategy can be extended directly to Z-pinned laminates with arbitrary stacking sequences, loading mode-mixities, different pin and laminate materials.

Acknowledgements

The authors would like to acknowledge Rolls-Royce plc for the support of this research through the Composites University Technology Centre (UTC) at the University of Bristol, UK.

References

[1] Cox, B.N. Constitutive Model for a Fiber Tow Bridging a Delamination Crack. *Mechanics of Composite Materials and Structures*, 6(2), pp.117–138, 1999.
[2] Cox, B.N. & Sridhar, N. A Traction Law for Inclined Fiber Tows Bridging Mixed-Mode Cracks. *Mechanics of Advanced Materials and Structures*, 9(4), pp.299–331, 2002.
[3] Allegri, G. & Zhang, X. On the delamination and debond suppression in structural joints by Z-fibre pinning. *Composites Part A: Applied Science and Manufacturing*, 38(4), pp.1107–1115, 2007.
[4] Dantuluri, V. et al. Cohesive modeling of delamination in Z-pin reinforced composite laminates. *Composites Science and Technology*, 67(3-4), pp.616–631, 2007.
[5] Dickinson, L.C., Farley, G.L. & Hinders, M.K. Prediction of Effective Three-Dimensional Elastic Constants of Translaminar Reinforced Composites. *Journal of Composite Materials*, 33(11), pp.1002–1029, 1999.
[6] Mouritz, a. P. Review of z-pinned composite laminates. *Composites Part A: Applied Science and Manufacturing*, 38(12), pp.2383–2397, 2007.
[7] Yasaee, M. et al. Experimental characterisation of mixed mode traction-displacement relationships for a single carbon composite Z-pin. *Composites Science and Technology*, 94, pp.123-131, 2014.
[8] Partridge, I.K. & Cartié, D.D.R. Delamination resistant laminates by Z-Fiber® pinning: Part I manufacture and fracture performance. *Composites Part A: Applied Science and Manufacturing*, 36(1), pp.55–64, 2005.
[9] Harper, P.W. & Hallett, S.R. Cohesive zone length in numerical simulations of composite delamination. *Engineering Fracture Mechanics*, 75(16), pp.4774–4792, 2008.
[10] Weibull, W. Weibull-ASME-Paper-1951.pdf. *Journal of Applied Mechanics*, 18(3), pp.293–297, 1951.
[11] Zhang, B., Allegri, G. & Hallett, S.R. Micro-Mechanical Finite Element Analysis of Single Z-pin Pull-out. *2013 SIMULIA UK Regional User Meeting*, pp.1–12, 2013.
[12] Sweeting, R.D. & Thomson, R.S. The effect of thermal mismatch on Z-pinned laminated composite structures. *Composite Structures*, 66(1-4), pp.189–195, 2004.
[13] Cox, B.N. Snubbing Effects in the Pullout of a Fibrous Rod from a Laminate. *Mechanics of Advanced Materials and Structures*, 12(2), pp.85–98, 2005.